The Journal of Immunology

Sex-Based Differences in Susceptibility to Severe Acute Respiratory Syndrome Coronavirus Infection

Rudragouda Channappanavar, Craig Fett, Matthias Mack, Patrick P. Ten Eyck, David K. Meyerholz and Stanley Perlman

J Immunol published online 3 April 2017
http://www.jimmunol.org/content/early/2017/04/04/jimmunol.1601896

The Journal of Immunology is published twice each month by
The American Association of Immunologists, Inc.,
1451 Rockville Pike, Suite 650, Rockville, MD 20852

Print ISSN: 0022-1767 Online ISSN: 1550-6606.

Published April 5, 2017, doi:10.4049/jimmunol.1601896

Sex-Based Differences in Susceptibility to Severe Acute Respiratory Syndrome Coronavirus Infection

Rudragouda Channappanavar,* Craig Fett,* Matthias Mack,† Patrick P. Ten Eyck,‡ David K. Meyerholz,§ and Stanley Perlman*

Pathogenic human coronaviruses (CoVs), such as the severe acute respiratory syndrome (SARS)-CoV and the Middle East respiratory syndrome–CoV, cause acute respiratory illness. Epidemiological data from the 2002–2003 SARS epidemic and recent Middle East respiratory syndrome outbreak indicate that there may be sex-dependent differences in disease outcomes. To investigate these differences, we infected male and female mice of different age groups with SARS-CoV and analyzed their susceptibility to the infection. Our results showed that male mice were more susceptible to SARS-CoV infection compared with age-matched females. The degree of sex bias to SARS-CoV infection increased with advancing age, such that middle-aged mice showed much more pronounced differences compared with young mice. Enhanced susceptibility of male mice to SARS-CoV was associated with elevated virus titers, enhanced vascular leakage, and alveolar edema. These changes were accompanied by increased accumulation of inflammatory monocyte macrophages and neutrophils in the lungs of male mice, and depletion of inflammatory monocyte macrophages partially protected these mice from lethal SARS. Moreover, the sex-specific differences were independent of T and B cell responses. Furthermore, ovariectomy or treating female mice with an estrogen receptor antagonist increased mortality, indicating a protective effect for estrogen receptor signaling in mice infected with SARS-CoV. Together, these data suggest that sex differences in the susceptibility to SARS-CoV in mice parallel those observed in patients and also identify estrogen receptor signaling as critical for protection in females. ***The Journal of Immunology*****, 2017, 198: 000–000.**

Pathogenic coronaviruses (CoVs), such as severe acute respiratory syndrome (SARS)-CoV and Middle East respiratory syndrome (MERS)-CoV and newly identified SARS- and MERS-like CoVs pose a significant threat to public health (1–7). SARS-CoV and MERS-CoV infect airway and alveolar epithelial cells and cause acute respiratory illnesses (8, 9). High initial virus loads and increased numbers of inflammatory monocyte macrophages (IMMs) and neutrophils in the lungs, associated with elevated proinflammatory cytokine/chemokine levels, caused lung damage in SARS patients (8, 10–12). The deleterious clinical manifestations of SARS likely stem from exuberant innate immune responses and virus-induced direct cytopathic effects (6, 13–15). Recent studies from our laboratory showed that robust virus replication accompanied by delayed type I IFN signaling resulted in inflammatory responses and lung immunopathology, with diminished survival in susceptible BALB/c mice (16).

*Department of Microbiology, University of Iowa, Iowa City, IA 52242; †Department of Internal Medicine, University Hospital Regensburg, Regensburg 93042, Germany; ‡Institute for Clinical and Translational Science, University of Iowa, Iowa City, IA 52242; and §Department of Pathology, University of Iowa, Iowa City, IA 52242

ORCIDs: 0000-0002-5041-0708 (P.P.T.E.); 0000-0003-4213-2354 (S.P.).

Received for publication November 7, 2016. Accepted for publication March 10, 2017.

This work was supported in part by the National Institutes of Health (Grants P01 AI060699 and R01 AI091322).

Address correspondence and reprint requests to Dr. Stanley Perlman, Department of Microbiology, BSB 3-712, University of Iowa, Iowa City, IA 52242. E-mail address: stanley-perlman@uiowa.edu

The online version of this article contains supplemental material.

Abbreviations used in this article: B6, C57BL/6; CFR, case fatality rate; CoV, coronavirus; IMM, inflammatory monocyte macrophage; MERS, Middle East respiratory syndrome; PI, perivascular inflammation; p.i., postinfection; SARS, severe acute respiratory syndrome.

Studies from the 2002–2003 SARS epidemic showed that individuals <25 y of age experienced mild to moderate illness. In contrast, elderly individuals aged ≥60 y suffered worse outcomes, with >50% mortality (8, 14). Similarly, young (6–wk-old) C57BL/6 (B6) mice were completely resistant to infection with mouse-adapted SARS-CoV (MA15); however, as mice aged, there was a steep increase in the susceptibility, such that mice older than 5 mo of age were highly susceptible to MA15 infection (17–19). In addition to age-dependent disease susceptibility, epidemiological studies showed sex-specific differences in the incidence and case fatality rates (CFRs) in humans after SARS-CoV infection, with males experiencing higher CFRs compared with females (20, 21). Similarly, data from recent MERS outbreaks showed high incidence and CFRs among men (22). This sex-dependent increase in disease severity after pathogenic CoV infection was more pronounced with advancing age (20, 22).

Males and females respond differently to many RNA and DNA virus infections (23). In general, males generate less robust immune responses and are more susceptible to a variety of infectious agents (23–27). In contrast, females mount stronger innate and adaptive immune responses and are relatively resistant to virus infections (23, 28–30). However, robust immune responses in females may also lead to immunopathology, resulting in fatal outcomes (23, 29, 31). Sex-specific disease outcomes following virus infections are attributed to sex-dependent production of steroid hormones, different copy numbers of immune response X-linked genes, and the presence of disease-susceptibility genes in males and females (23, 32). Although testosterone suppresses innate immune responses, hormones such as estrogens have disparate functions, with an immune-suppressive effect at high concentrations and immunostimulatory activity at low concentrations (23, 24, 33, 34). Estrogen signaling also promotes adaptive T cell responses in female mice by increasing neutrophil accumulation (30). Additionally, a recent study demonstrates a direct role for estrogen signaling in limiting

influenza virus replication in nasal epithelial cells derived from humans by modulating genes that regulate the metabolic functions of cells (35).

Although the epidemiological data from SARS and MERS outbreaks show male bias in disease susceptibility (20, 22), the basis for the differential susceptibility has not been established. Using a mouse model of SARS-CoV infection, we show that male mice are more susceptible to SARS-CoV infection than female mice. The enhanced susceptibility of male mice to SARS-CoV correlates with a moderate increase in virus titer and extensive IMM and neutrophil accumulation in the lungs. Furthermore, although gonadectomy did not affect disease outcome in male mice, ovariectomy or treating female mice with estrogen receptor antagonist ICI 182, 780 resulted in increased mortality to SARS-CoV infection, suggesting that estrogen signaling protects female mice from a lethal MA15 infection.

Materials and Methods

Mice and viruses

Specific pathogen–free male and female B6 and BALB/c mice (8–9 wk, 5 and 8–10 mo) (Charles River) and 18–20-mo male and female B6 mice (National Institute on Aging aging colony) were bred and maintained in the University of Iowa animal care facility. The University of Iowa Institutional Animal Care and Use Committee approved all animal experiments. Mouse-adapted SARS-CoV (MA15), a kind gift from K. Subbarao (National Institutes of Health, Bethesda, MD), was propagated on Vero E6 cells. Mice were lightly anesthetized using isoflurane and were intranasally infected with different doses of SARS-CoV in 50 μl of DMEM. In preliminary experiments, we showed that the use of isoflurane, an inhalant, and ketamine/xylazine, an injectable anesthetic, gave similar results after SARS-CoV infection (Supplemental Fig. 1A). All work with infectious SARS-CoV was performed in Centers for Disease Control and Prevention/Biological Select Agents and Toxin–Registered Biosafety Level 3 and Animal Biosafety Level 3 laboratories.

Virus titers in the lungs and preparation of lung cells for FACS analyses

Lung virus titers were determined on the Vero E6 cell line, as described earlier (17). FACS staining for lung cells was carried out as previously described (16, 17). Briefly, mice were sacrificed at the indicated time points. The lungs were perfused via the right ventricle with 10 ml of PBS, and the lungs were removed, cut into small pieces, and digested in HBSS buffer containing 2% FCS, 25 mM HEPES, 1 mg/ml Collagenase D (Roche), and 0.1 mg/ml DNase (Roche) for 30 min at room temperature. Digested lungs were minced, and the cell suspension was passed through a 70-μm strainer. Cells were then incubated with CD16/32, washed, and stained with fluorochrome-conjugated cell surface Abs.

Vascular leakage

Infected and control male and female mice were injected i.v. with 200 μl of Evan's blue dye (1.0% in PBS) on day 4 postinfection (p.i.). After 30 min, mice were anesthetized, and lungs were perfused with a 10-ml intracardial injection of PBS (36).

Abs and flow cytometry

For surface/intracellular staining, cells were incubated with the following fluorochrome-labeled Abs specific for mouse: PECy7–anti-CD45 (30-F11), FITC–anti-Ly6G (1A8), PE/PerCp-Cy5.5–anti-Ly6C (AL-21), V450–anti-CD11b (M1/70), allophycocyanin–anti-F4/80 (BM8), FITC/PE–anti-CD11c (HL3), anti-CD80 (16-10A1), anti-CD4 (RM4-5), anti-CD8α (53-6.7), allophycocyanin–anti-TNF-α (MP6-XT22), allophycocyanin–anti-IL-6 (MP5-20F3), allophycocyanin–anti-IL-β (NJTEN3), and allophycocyanin–anti-iNOS (CXNFT) (BD Biosciences or eBioscience). Intracellular cytokine staining was carried out using a previously described protocol (16).

RNA preparation from lungs and cytokine/chemokine estimation by quantitative PCR

RNA was extracted from the lungs of mice (TRIzol; Invitrogen), and mRNA levels were determined after normalizing each sample to HPRT. Specific primer sets used for quantitative PCR were described previously (16).

Lung histology and immunohistochemistry

Lungs were removed, fixed in zinc formalin, and embedded in paraffin, and tissue sections were stained with H&E. Lung tissues were analyzed using the postexamination method of masking on tissue sections. Tissues were scored based on the extent of edema in lung air spaces using the following grades: 0, absence of edema; 1, edema detected in <33% of lung; 2, edema detected in 34–66% of lung; and 3, edema detected in >66% of lung. Tissues were also scored for the extent of perivascular inflammation (PI) using the following scale: 0, absence of PI; 1, mild PI aggregates around rare (fewer than three) vessels; 2, moderate PI aggregates around vessels (three to five vessels); and 3, moderate to expansile PI aggregates around vessels (more than five vessels). Scores were evaluated using Prism software and the Mann–Whitney U test, with $p = 0.05$ as a threshold for significance.

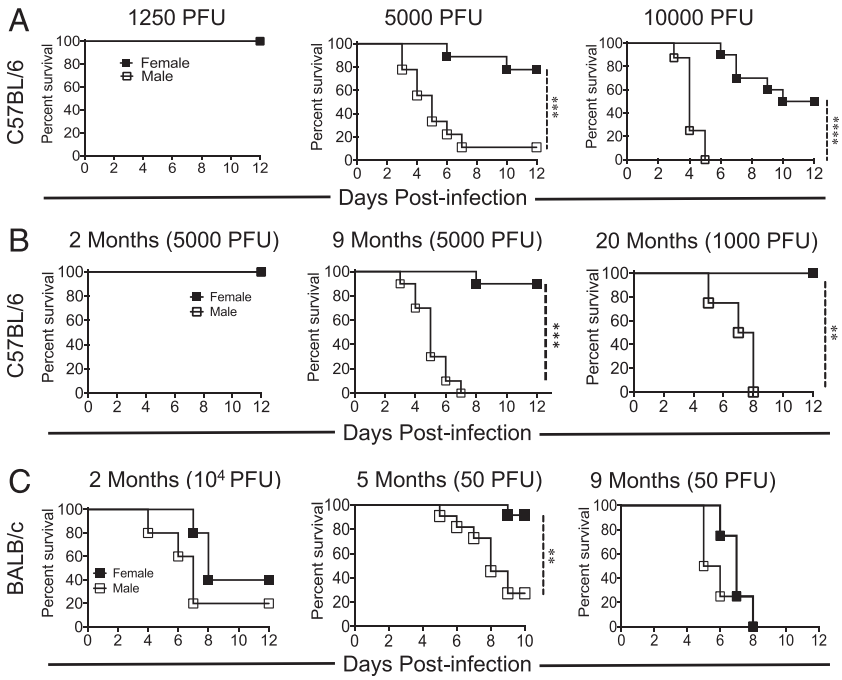

FIGURE 1. Male mice are more susceptible to MA15 infection than female mice. (**A**) Nine-month-old male and female mice were infected with 1250, 5000, or 10^4 PFU MA15, and survival was monitored for 12 d. (**B**) Two- and nine-month-old B6 male and female mice were infected with 5000 PFU MA15, and 18–20-mo-old B6 mice were challenged with 1000 PFU MA15. Survival was monitored for 12 dpi. (A and B) Data are derived from two independent experiments with four or five mice per group per experiment. (**C**) Two-month-old BALB/c mice and 5- and 9-mo-old BALB/c mice were infected with 10^4 and 50 PFU MA15, respectively, and were monitored for morbidity and mortality. Data are derived from two or three independent experiments with three to five mice per group per experiment (left and middle panels) and from one experiment with four or five mice per group (right panel). $^{**}p < 0.01$, $^{***}p < 0.001$, $^{****}p < 0.0001$, log-rank test with 95% CI.

Viral Ag was detected using rabbit anti-N protein (1:1000) (IMG548; Imgenex), followed by labeling with biotinylated goat anti-rabbit IgG (1:200). Samples were developed with 3,3'-diaminobenzidine for 3 min.

IMM-depletion studies

Eight- to ten-month-old male and female B6 mice were treated i.p. with anti-CCR2 Ab (clone MC21, 25 μg per mouse, i.p. in 250 μl PBS) at −6 h and at day 1 p.i. (16).

Treatment with flutamide, tamoxifen, and ICI 182, 780

Male mice (8–9 mo) were treated with flutamide (20 mg/kg, in corn oil, s.c.) on days −6, −4, −2, and 0 of MA15 infection. Female mice (8–9 mo) were treated with tamoxifen (1 mg per mouse, i.p.) or ICI 182, 780 (1 mg per mouse, i.p.) in corn oil on days −6, −4, −2, and 0 p.i. Equal volumes of corn oil were used as vehicle control (37). Mice were infected with 5000 PFU MA15. Of note, ICI 182, 780 treatment did not change the serum estradiol levels in naive female mice (Supplemental Fig. 1B).

Quantitation of serum estrogen levels

Serum estradiol concentration was measured by ELISA, as per the manufacturer's instructions (Enzo Life Sciences).

Statistical analysis

Statistical significance for survival studies was calculated using the log-rank (Mantel–Cox) test with 95% confidence interval (CI). Statistical analyses for the rest of the figures (Figs. 2, 3, 4A, 4C, 7A, 7C) fall under the generalized linear modeling framework. Similar to a two-way ANOVA, all models considered contained two main effects variables along with their interaction term. Because the outcome variables generally followed a right-skewed distribution, we used a log-link function so that the modeling assumptions are appropriately satisfied by the data. In all models, time period was one of the two main effects. The other variable is the comparison of interest (i.e., sex, titer, or group). In some analyses, data sets cover multiple strata, so we fit each model to obtain estimates for each level of the variable of interest for each time point within each stratum. The comparisons at each time point are estimated and have corresponding p values, which can be used to determine statistical significance by comparing to the cutoff value $\alpha = 0.05/n$ (n is the number of comparisons made within a time point and stratum).

Results

Male mice are highly susceptible to SARS-CoV infection

To examine sex-specific differences following SARS-CoV infection, we initially infected 8–10-mo-old male and female B6 mice with different doses of MA15 and monitored morbidity and mortality (Fig. 1A). Male and female mice infected with 1250 PFU MA15 were completely protected from SARS. However, increasing the MA15 infection dose to 5000 PFU resulted in ~90% mortality in male mice compared with ~20% mortality in females (Fig. 1A). Further, at 10^4 PFU, all male mice died, whereas ~40% of the females survived MA15 infection (Fig. 1A). Because CFRs of men and women varied with age following SARS-CoV and MERS-CoV infection (20, 22), we then investigated whether sex-specific differences in disease outcomes were age dependent. For

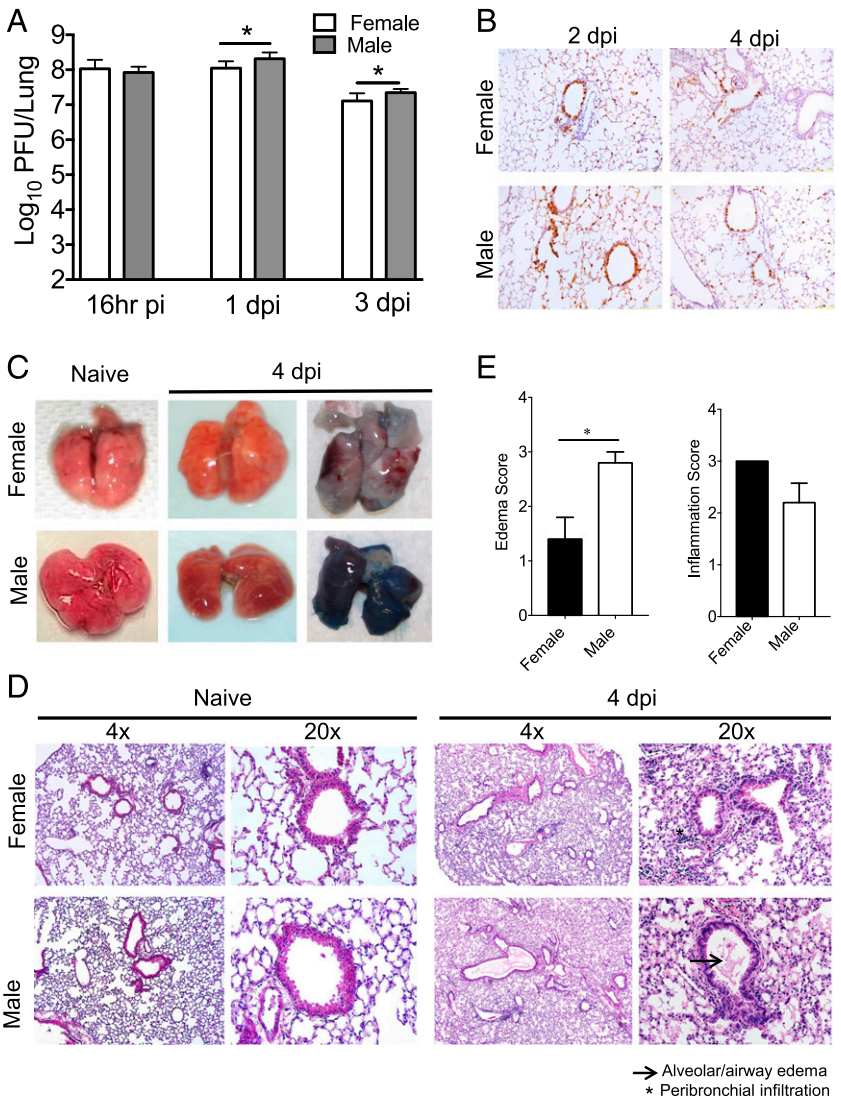

FIGURE 2. Virus titers and lung pathology in MA15-infected mice. Nine-month-old male and female mice were infected with 5000 PFU MA15, and lungs were analyzed for titer (**A**), viral Ag staining in the lungs at different times p.i. (original magnification ×10) (**B**), gross pathology and vascular leakage in lungs of naive and MA15-infected male and female mice on day 4 p.i. (**C**), and histology in naive and MA15-infected male and female mice on day 4 p.i. (**D**). (**E**) Lung inflammation and edema scores were determined at day 4 p.i. These data are derived from four or five mice per group. (A) Data are representative of two independent experiments. Statistical significance was determined as described in *Materials and Methods*. $*p < 0.05$.

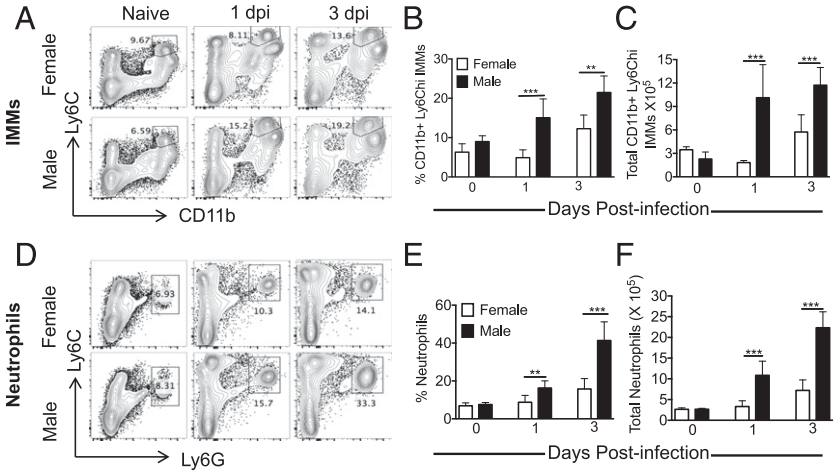

FIGURE 3. Increased IMM accumulation in the lungs of MA15-infected male mice. Mice were infected with 5000 PFU MA15 and analyzed for IMMs (**A**–**C**) or neutrophils (**D**–**F**) in the lungs on days 0, 1, and 3 p.i. Representative FACS plots show the percentage of IMMs (A) and neutrophils (D) in the lings. Bar graphs show the percentage and total number of IMMs (B and C) and neutrophils (E and F) at different time p.i. Data are representative of two independent experiments with four mice per group per experiment. Statistical significance was determined as described in *Materials and Methods*. $^{**}p < 0.01$, $^{***}p < 0.001$.

these experiments, male and female mice of different age groups were challenged with 5000 PFU MA15 virus. As shown in Fig. 1B, young 2-mo-old male and female mice were completely resistant to developing SARS. Conversely, all 8–9-mo-old male mice succumbed to MA15 infection, whereas only 10% of females died of the infection. Although all aged (20 mo) mice succumbed to infection

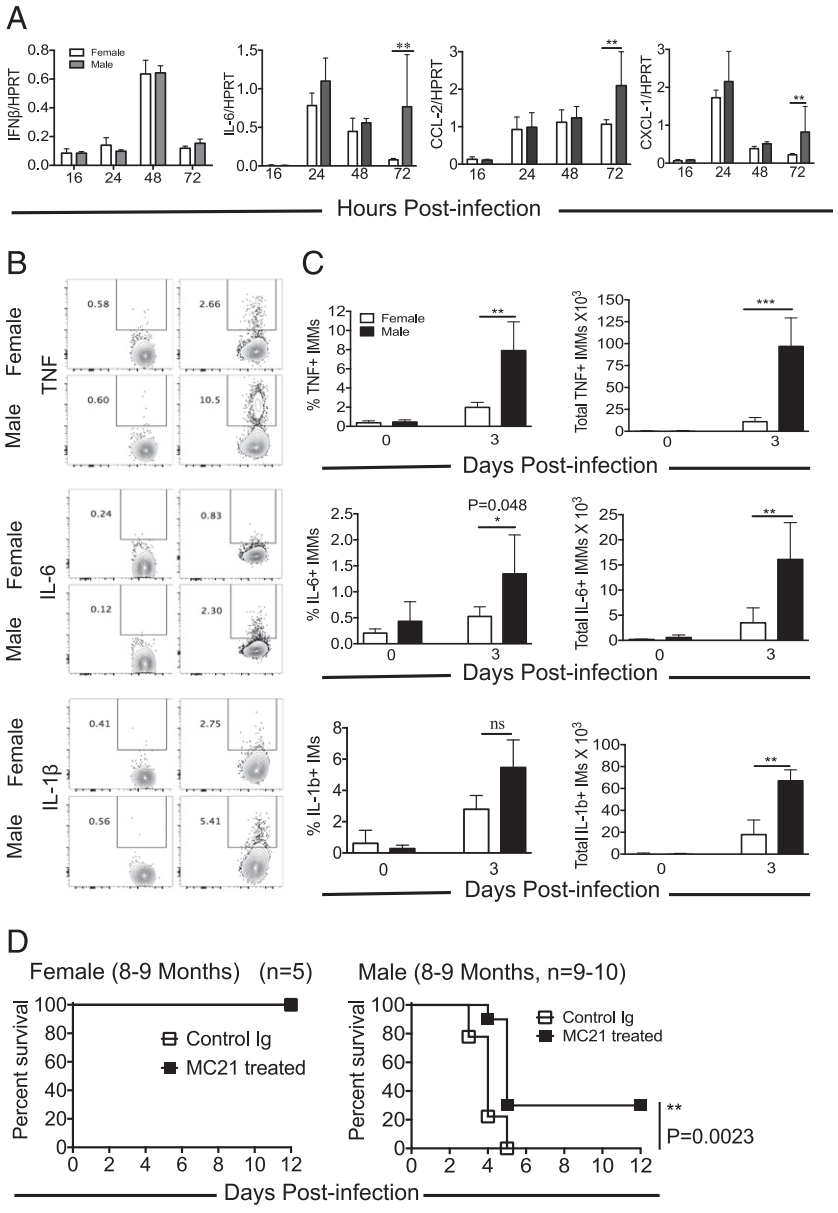

FIGURE 4. Enhanced proinflammatory cytokines/chemokines in the lungs of MA15-challenged male mice. Eight- to nine-month-old male and female mice were infected with 5000 PFU MA15. (**A**) mRNA levels of antiviral and proinflammatory cytokines/chemokines in the lungs were measured at different times p.i. Data were obtained from four or five mice per group. FACS plots (**B**) and bar graphs (**C**) show the percentage and number of cytokine-producing IMMs in the lungs of male and female mice on day 3 p.i. following a 7-h ex vivo incubation in the presence of brefeldin A. (**D**) Nine-month-old female and male mice were treated with control Ig or MC21 Ab (anti-CCR2, depletes IMMs) at −6 h and day 1. These mice were infected with 4000 PFU MA15, and survival was recorded. (B–D) Data represent two independent experiments with four or five mice per group per experiment. Statistical significance was determined as described in *Materials and Methods*. $^{*}p < 0.05$, $^{**}p < 0.01$, $^{***}p < 0.001$. ns, not significant.

with 5000 PFU MA15, male mice succumbed to infection with 1000 PFU MA15, whereas all female mice survived (Fig. 1B).

To determine whether sex-specific disease outcomes after MA15 challenge were limited to B6 mice, we infected young (8–9 wk), adult (5 mo), and middle-aged (8–9 mo) BALB/c mice with MA15 (Fig. 1C). BALB/c mice exhibit striking age-dependent differences in morbidity and mortality, so we used lower doses of MA15 in older mice to identify sex-specific disease outcomes. Similar to B6 mice, there was no difference in the susceptibility of young male and female BALB/c mice to MA15 challenge. However, 5-mo-old adult male BALB/c mice were highly susceptible in comparison with age-matched female mice when infected with 50 PFU MA15. Sex-specific differences in 9-mo-old mice could not be discerned because both male and female mice were highly susceptible to MA15 infection, even at a low dose (50 PFU) (Fig. 1C). Together, these results show that males are more susceptible to MA15 infection than are female mice.

Enhanced virus replication and lung pathology in male mice

Because sex-specific disease outcomes were most pronounced in middle-aged mice, we used 8–9-mo-old male and female B6 mice for further studies. We first determined virus titers in the lungs of MA15-infected male and female mice. Total virus loads were nearly identical in the lungs at 16 h p.i.; however, we observed a modest increase (2–3-fold) in MA15 titer in the lungs of male mice compared with females at days 1 and 3 p.i. (Fig. 2A). SARS–CoV–N Ag was detected in airway epithelial cells and in type I and II pneumocytes in male and female mice at days 2 and 4 p.i. Moderately greater viral Ag staining was noted in the lung airways and parenchyma of male mice (Fig. 2B). Gross examination of the lungs revealed extensive hyperemia and congestion in male mice at day 4 p.i., whereas those from female mice appeared nearly normal (Fig. 2C). Additionally, lung vascular leakage was much more prominent in SARS-CoV–infected male mice, as assessed in an Evans Blue extravasation assay at day 4 p.i. (Fig. 2C, right panels). Further, histological examination of lungs revealed marked alveolar edema and terminal bronchiolar epithelial sloughing in male mice at day 4 p.i., whereas female lungs showed minimal alveolar edema with increased peribronchial–perivascular immune cell infiltration (Fig. 2D, 2E). These results show a marginal, but significant, increase in virus replication with pronounced gross and microscopic pathological changes in male mice.

Increased accumulation of IMMs and neutrophils in the lungs of male mice

Next, we investigated whether sex-specific disease susceptibility in males correlated with increased inflammatory cell recruitment. Total lung cells harvested from MA15-infected 8–9-mo-old male and female mice were analyzed for the percentage and total

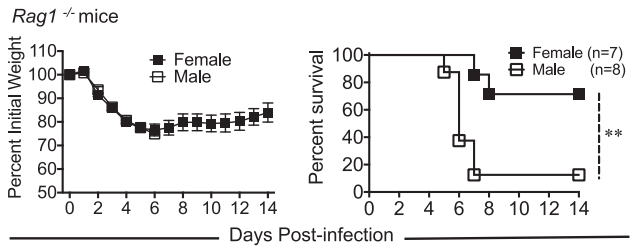

FIGURE 5. Enhanced susceptibility of male mice to MA15 infection is independent of T and B cell response. Seven-to eight-month-old male and female RAG1$^{-/-}$ mice were challenged with 1750 PFU MA15 and monitored for morbidity and mortality for 14 d. Data are derived from seven or eight mice per group. $^{**}p < 0.01$, log-rank test with 95% CI.

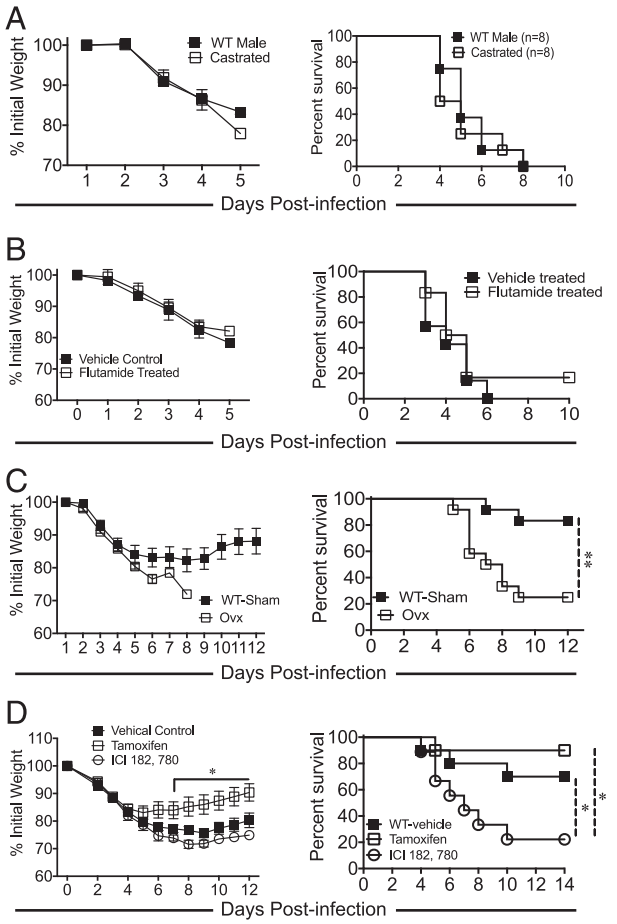

FIGURE 6. Estrogen receptor signaling protects female mice from lethal MA15 infection. Nine- to ten-month-old male and female and their gonadectomized counterparts were infected with 5000 PFU MA15. Nine-month old gonadectomized ($n = 8$) or nongonadectomized ($n = 8$) (**A**) and control ($n = 6$) or flutamide-treated ($n = 7$) (**B**) male mice were monitored for disease severity. (**C**) Percentage of initial weight and survival among control ($n = 12$) or ovariectomized female ($n = 12$) mice. (**D**) Female mice treated with vehicle (corn oil; $n = 9$), tamoxifen (1 mg per mouse; $n = 9$–10), or ICI 182, 780 (1 mg per mouse; $n = 10$) in 100 μl of corn oil were infected with 5000 PFU MA15 and monitored for morbidity and mortality. Data are derived from two or three independent experiments with three to five mice per group per experiment. $^{*}p < 0.05$, $^{**}p < 0.01$, log-rank test with 95% CI.

number of different innate immune cells. Total numbers of alveolar macrophages, NK cells, and plasmacytoid dendritic cells were nearly the same in MA15-infected male and female lungs at days 1 and 3 p.i. (data not shown). In contrast, significantly increased numbers of Ly6C^{hi}CD11b^{+} IMMs and neutrophils infiltrated into the lungs of male mice compared with females on days 1 and 3 p.i. (Fig. 3). At day 3 p.i., 2–3-fold more IMMs were present in the lungs of male mice compared with female mice (Fig. 3A–C). Similarly, a 4–5-fold increase in the total number of neutrophils was noted in the lungs of male mice at days 1 and 3 p.i. (Fig. 3C, 3D, and 3F).

Inflammatory cytokine and chemokine activity in the lungs of male and female mice

Increased mortality in male mice may result from an exuberant, but ineffective, cytokine response. To evaluate this possibility, we analyzed cytokine mRNA at different times post-MA15 infection. As shown in Fig. 4A, transcript levels of IFN-β were similar in male and female lungs at different times post-MA15 infection. In

contrast, mRNA levels of proinflammatory cytokines (IL-6) and chemokines (CCL2 and CXCL1), which were equivalent in both sexes early p.i., were upregulated in the lungs of male mice compared with females at day 3 p.i. (Fig. 4A), suggesting a more robust inflammatory response. Next, to determine whether the disparate proinflammatory cytokine/chemokine levels in the lungs were due to altered cytokine and chemokine production by IMMs, lung IMMs harvested from MA15-infected male and female mice at day 3 p.i. were stained directly ex vivo for intracellular TNF, IL-6, and IL-1β without stimulation in vitro. Intracellular cytokine analyses showed that significantly higher frequencies and numbers of IMMs expressed proinflammatory cytokines in male mice compared with female mice (Fig. 4B, 4C). To investigate whether accumulating IMMs were, in fact, responsible for the increased mortality observed in 8–9-mo-old male mice, we depleted IMMs in female and male mice using MC21 Ab, as described previously (16). mAb MC21 targets CCR2 and specifically depletes IMMs. As expected, depletion of IMM did not affect disease outcome in female B6 mice (Fig. 4D). However, mAb MC21 Ab treatment provided marginal, but significant, protection in 8–9-mo-old male mice (Fig. 4D), suggesting that IMMs contributed to lethal disease in male mice.

Sex-dependent SARS outcomes are independent of adaptive immunity

Most 8–9-mo-old B6 male mice succumbed to MA15 infection between days 5 and 7 p.i., a time that correlates with peak T cell responses after MA15 infection. To examine whether a differential adaptive immune response to MA15 infection contributed to increased disease in male mice, we examined MA15-induced morbidity and mortality in 8-mo-old male and female RAG1$^{-/-}$ mice, which lack mature T and B cells. As shown in Fig. 5, male and female RAG1$^{-/-}$ mice lost equivalent weight after MA15 infection. However, mortality was significantly higher in male RAG1$^{-/-}$ male compared with female mice, suggesting that disease outcomes were independent of T cell and Ab responses.

Estrogen signaling protects female mice from lethal MA15 infection

We next investigated the role of sex steroids in SARS-CoV pathogenesis by comparing gonadectomized and control counterparts p.i. Gonadectomy or treatment with flutamide, a nonsteroidal anti-androgen, did not affect morbidity and mortality in male mice following lethal MA15 infection, suggesting that androgens do not play a role in SARS-CoV pathogenesis (Fig. 6A, 6B). However, a caveat of these experiments is that SARS-CoV infection significantly reduces serum testosterone levels (data not shown). In marked contrast, MA15-infected gonadectomized female mice showed progressive weight loss, and ~85% died by day 8 p.i., whereas only 10–20% mortality was observed in control female mice (Fig. 6C). Furthermore, female mice treated with the estrogen receptor antagonist ICI 182, 780 were more susceptible to MA15 infection compared with female mice treated with estrogen receptor agonist/modulator, tamoxifen, or vehicle control (Fig. 6D). Notably, female mice treated with tamoxifen showed significantly reduced weight loss compared with vehicle control–treated mice after MA15 infection (Fig. 6D). These results demonstrated that estrogen receptor signaling protected female mice from MA15 infection, whereas androgens did not influence disease outcome in males.

Increased IMM accumulation in ovariectomized female mice

To determine whether the lack of estrogen signaling was sufficient to cause the same changes in the immune response that was observed in males, we examined viral titers, and IMM and neutrophil

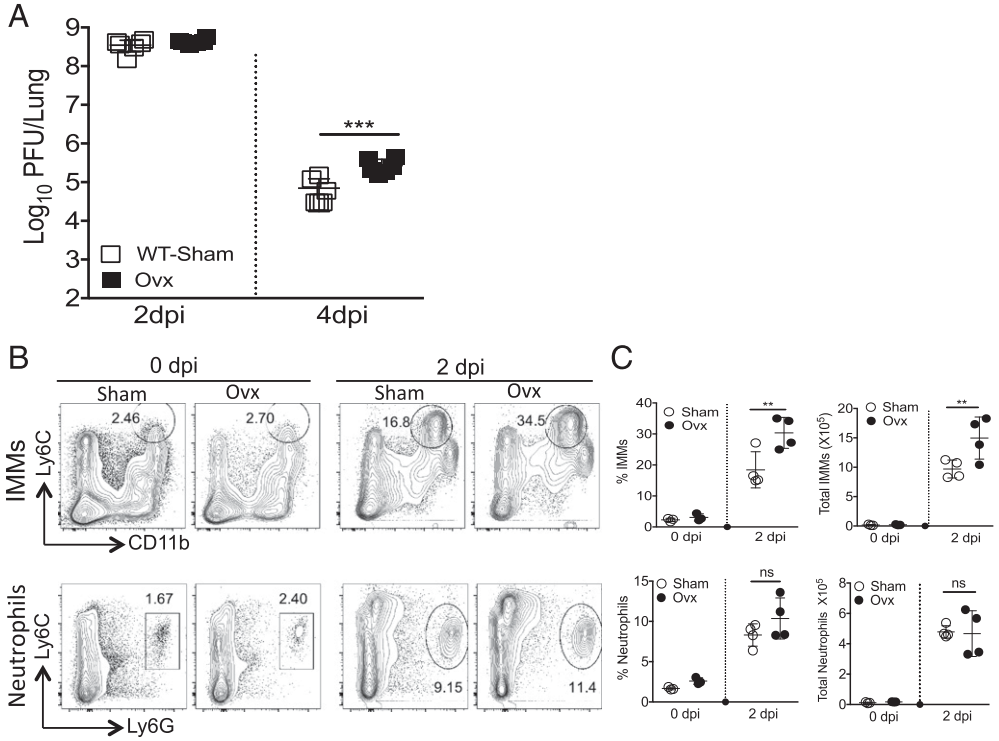

FIGURE 7. Virus titer and IMM accumulation in ovariectomized female mice. Nine-month old control or ovariectomized mice were infected with 5000 PFU MA15, and virus titers and inflammatory cell accumulation were analyzed. (**A**) Lung virus titers in 9-mo-old male and female mice at days 2 and 4 p.i. (**B** and **C**) IMM and neutrophil accumulation in the lungs at day 2 p.i. Data are derived from two independent experiments with three or four mice per group per experiment (A) or are representative of two independent experiments with three or four mice per group per experiment (B and C). Statistical significance was determined as described in *Materials and Methods*. $^{**}p < 0.01$, $^{***}p < 0.001$. ns, not significant.

accumulation in control and ovariectomized female mice at different times post-MA15 infection. As shown in Fig. 7A, total lung MA15 titers were identical in both groups of mice at day 2 p.i., but marginally increased virus titers were noted on day 4 p.i. Additionally, lungs of ovariectomized mice showed an increased percentage and number of IMMs, but not neutrophils, at day 2 p.i. (Fig. 7B, 7C), suggesting a role for lung IMMs in disease severity, as we observed previously in another model of severe SARS (16). Thus, decreased estrogen signaling accounted for some, but not all, of the immune changes observed in MA15-infected male mice.

Discussion

Our results show that male mice are highly susceptible to SARS-CoV infection compared with age-matched females. These results are consistent with SARS and MERS studies in humans that showed a trend toward sex-specific disease outcomes in middle-aged individuals compared with younger individuals (20, 22). In agreement with the human studies, our results demonstrate that sex-specific differences in disease severity are prominent in middle-aged mice and are less prominent in young and aged mice (Fig. 1). Of note, differences were less apparent in individuals aged ≥75 y, possibly because of the enhanced mortality in all elderly, regardless of sex, due to dysregulated immune responses (38).

Multiple factors contribute to disparity in sex-specific disease outcomes following virus infections. Sex-specific steroids and activity of X-linked genes, both of which modulate the innate and adaptive immune response to virus infection, influence the immune response (23, 27, 39–41). High copy numbers of TLR7 (located on the X-chromosome) and elevated IRF-7 expression in females induce increased IFN-β production by plasmacytoid dendritic cells and provided protection against HIV infection (42, 43). Similarly, elevated type I IFN levels correlated with reduced mouse hepatitis virus titers in female mice compared with male mice, possibly through TLR7 activation (31). In the current study, mRNA levels of IFN-β were equivalent during all time points examined. However, although proinflammatory cytokine (IL-6) and chemokine (CCL2 and CXCL1) expression was similar in both sexes early (16, 24, and 48 h p.i.) after SARS-CoV challenge, the levels of these cytokines and chemokines remained elevated or even increased in the lungs of male mice compared with females at 72 h p.i. (Fig. 4A), suggesting a prolonged inflammatory response in male mice.

Estrogens are known to suppress monocyte–macrophage recruitment by downregulating CCL2 expression during inflammation and inhibiting TLR4-mediated NFκβ activation in macrophages via suppression of micro-RNAs, such as let7a and miR-125b (44, 45). Similarly, treating gonadectomized mice with estrogen reduced the levels of TNF and CCL2 and, thus, protected them from influenza virus infection (29, 30). We recently showed that IMMs were the predominant source of these proinflammatory cytokines and chemokines during lethal SARS (16). In the current study, we observed increased numbers of IMMs and neutrophils in SARS-CoV–infected males. Additionally, increased numbers of IMMs correlated with elevated levels of proinflammatory cytokines and chemokines in the lungs of male mice, and these cells also produced more of these inflammatory mediators in male mice compared with female mice (Fig. 4). Further, increased numbers of IMMs in ovariectomized mice compared with intact female mice suggest that estrogen signaling in females suppressed the accumulation and function of IMMs in the lungs. We also identified a pathogenic role for type I IFN during SARS-CoV infection (16). Rapid SARS-CoV replication accompanied by delayed type I IFN signaling promoted the accumulation of pathogenic IMMs, resulting in elevated lung cytokine/chemokine levels, vascular leakage, and an impaired T cell response (16). However, no detectable difference in IFN-β levels in the lungs of male and female mice suggest that the basis for the differences is IFN independent in this instance. Additionally, it is unlikely that impaired virus-specific T cell responses resulted in enhanced SARS in males, because sex-specific disease outcomes were evident in T and B cell–deficient RAG1$^{-/-}$ mice.

Another factor that could contribute to differential outcomes in males and females is the direct cytopathic effect that is due to higher virus loads in males (6, 15). Estrogen treatment of cultured nasal epithelial cells isolated from naive female mice suppressed influenza A virus replication by modulating genes associated with cellular metabolism. In contrast, treating nasal epithelial cells isolated from male mice with estrogen had no effect on virus replication (35). Because SARS-CoV predominantly replicates in airways and alveolar epithelial cells (46), and estradiol concentrations are higher in female mice (47), estrogen signaling in females may directly suppress SARS-CoV replication via effects on cellular metabolism. Moreover, high viral RNA levels in the lungs of male mice may stimulate TLR7 on IMMs, resulting in elevated proinflammatory cytokines and chemokines (48).

Our results highlight sex-specific differences in susceptibility to SARS-CoV and perhaps other CoV infections. Higher virus titers and increased IMM and neutrophil infiltration in the lungs suggest the contribution of multiple factors to the disease severity observed in male mice. Additionally, enhanced susceptibility of ovariectomized and estrogen receptor antagonist–treated female mice demonstrate the protective effect of estrogen receptor signaling in females. Overall, the results are consistent with the sex bias observed in human CoV infections and provide mechanistic insight into the differences in disease severity in men and women.

Acknowledgments

We thank Dr. Anthony R. Fehr for careful review of the manuscript.

Disclosures

The authors have no financial conflicts of interest.

References

1. Zaki, A. M., S. van Boheemen, T. M. Bestebroer, A. D. Osterhaus, and R. A. Fouchier. 2012. Isolation of a novel coronavirus from a man with pneumonia in Saudi Arabia. *N. Engl. J. Med.* 367: 1814–1820.
2. Peiris, J. S., Y. Guan, and K. Y. Yuen. 2004. Severe acute respiratory syndrome. *Nat. Med.* 10(Suppl.): S88–S97.
3. Menachery, V. D., B. L. Yount, Jr., K. Debbink, S. Agnihothram, L. E. Gralinski, J. A. Plante, R. L. Graham, T. Scobey, X. Y. Ge, E. F. Donaldson, et al. 2015. A SARS-like cluster of circulating bat coronaviruses shows potential for human emergence. *Nat. Med.* 21: 1508–1513.
4. Alagaili, A. N., T. Briese, N. Mishra, V. Kapoor, S. C. Sameroff, P. D. Burbelo, E. de Wit, V. J. Munster, L. E. Hensley, I. S. Zalmout, et al. 2014. Middle East respiratory syndrome coronavirus infection in dromedary camels in Saudi Arabia. [Published erratum appears in 2014 *MBio* 5: e01002–14.] *MBio* 5: e00884–e14.
5. Ge, X. Y., J. L. Li, X. L. Yang, A. A. Chmura, G. Zhu, J. H. Epstein, J. K. Mazet, B. Hu, W. Zhang, C. Peng, et al. 2013. Isolation and characterization of a bat SARS-like coronavirus that uses the ACE2 receptor. *Nature* 503: 535–538.
6. Drosten, C., S. Günther, W. Preiser, S. van der Werf, H. R. Brodt, S. Becker, H. Rabenau, M. Panning, L. Kolesnikova, R. A. Fouchier, et al. 2003. Identification of a novel coronavirus in patients with severe acute respiratory syndrome. *N. Engl. J. Med.* 348: 1967–1976.
7. Kuiken, T., R. A. Fouchier, M. Schutten, G. F. Rimmelzwaan, G. van Amerongen, D. van Riel, J. D. Laman, T. de Jong, G. van Doornum, W. Lim, et al. 2003. Newly discovered coronavirus as the primary cause of severe acute respiratory syndrome. *Lancet* 362: 263–270.
8. Nicholls, J. M., L. L. Poon, K. C. Lee, W. F. Ng, S. T. Lai, C. Y. Leung, C. M. Chu, P. K. Hui, K. L. Mak, W. Lim, et al. 2003. Lung pathology of fatal severe acute respiratory syndrome. *Lancet* 361: 1773–1778.
9. Gu, J., E. Gong, B. Zhang, J. Zheng, Z. Gao, Y. Zhong, W. Zou, J. Zhan, S. Wang, Z. Xie, et al. 2005. Multiple organ infection and the pathogenesis of SARS. *J. Exp. Med.* 202: 415–424.

10. Franks, T. J., P. Y. Chong, P. Chui, J. R. Galvin, R. M. Lourens, A. H. Reid, E. Selbs, C. P. McEvoy, C. D. Hayden, J. Fukuoka, et al. 2003. Lung pathology of severe acute respiratory syndrome (SARS): a study of 8 autopsy cases from Singapore. *Hum. Pathol.* 34: 743–748.
11. Wong, C. K., C. W. Lam, A. K. Wu, W. K. Ip, N. L. Lee, I. H. Chan, L. C. Lit, D. S. Hui, M. H. Chan, S. S. Chung, and J. J. Sung. 2004. Plasma inflammatory cytokines and chemokines in severe acute respiratory syndrome. *Clin. Exp. Immunol.* 136: 95–103.
12. Jiang, Y., J. Xu, C. Zhou, Z. Wu, S. Zhong, J. Liu, W. Luo, T. Chen, Q. Qin, and P. Deng. 2005. Characterization of cytokine/chemokine profiles of severe acute respiratory syndrome. *Am. J. Respir. Crit. Care Med.* 171: 850–857.
13. van den Brand, J. M., B. L. Haagmans, D. van Riel, A. D. Osterhaus, and T. Kuiken. 2014. The pathology and pathogenesis of experimental severe acute respiratory syndrome and influenza in animal models. *J. Comp. Pathol.* 151: 83–112.
14. Chen, J., and K. Subbarao. 2007. The immunobiology of SARS*. *Annu. Rev. Immunol.* 25: 443–472.
15. Sims, A. C., R. S. Baric, B. Yount, S. E. Burkett, P. L. Collins, and R. J. Pickles. 2005. Severe acute respiratory syndrome coronavirus infection of human ciliated airway epithelia: role of ciliated cells in viral spread in the conducting airways of the lungs. *J. Virol.* 79: 15511–15524.
16. Channappanavar, R., A. R. Fehr, R. Vijay, M. Mack, J. Zhao, D. K. Meyerholz, and S. Perlman. 2016. Dysregulated type I interferon and inflammatory monocyte-macrophage responses cause lethal pneumonia in SARS-CoV–infected mice. *Cell Host Microbe* 19: 181–193.
17. Zhao, J., J. Zhao, K. Legge, and S. Perlman. 2011. Age-related increases in PGD (2) expression impair respiratory DC migration, resulting in diminished T cell responses upon respiratory virus infection in mice. *J. Clin. Invest.* 121: 4921–4930.
18. Frieman, M., B. Yount, S. Agnihothram, C. Page, E. Donaldson, A. Roberts, L. Vogel, B. Woodruff, D. Scorpio, K. Subbarao, and R. S. Baric. 2012. Molecular determinants of severe acute respiratory syndrome coronavirus pathogenesis and virulence in young and aged mouse models of human disease. *J. Virol.* 86: 884–897.
19. Roberts, A., C. Paddock, L. Vogel, E. Butler, S. Zaki, and K. Subbarao. 2005. Aged BALB/c mice as a model for increased severity of severe acute respiratory syndrome in elderly humans. *J. Virol.* 79: 5833–5838.
20. Karlberg, J., D. S. Chong, and W. Y. Lai. 2004. Do men have a higher case fatality rate of severe acute respiratory syndrome than women do? *Am. J. Epidemiol.* 159: 229–231.
21. Leong, H. N., A. Earnest, H. H. Lim, C. F. Chin, C. Tan, M. E. Puhaindran, A. Tan, M. I. Chen, and Y. S. Leo. 2006. SARS in Singapore–predictors of disease severity. *Ann. Acad. Med. Singapore* 35: 326–331.
22. Alghamdi, I. G., I. I. Hussain, S. S. Almalki, M. S. Alghamdi, M. M. Alghamdi, and M. A. El-Sheemy. 2014. The pattern of Middle East respiratory syndrome coronavirus in Saudi Arabia: a descriptive epidemiological analysis of data from the Saudi Ministry of Health. *Int. J. Gen. Med.* 7: 417–423.
23. Klein, S. L., and K. L. Flanagan. 2016. Sex differences in immune responses. *Nat. Rev. Immunol.* 16: 626–638.
24. Rettew, J. A., Y. M. Huet-Hudson, and I. Marriott. 2008. Testosterone reduces macrophage expression in the mouse of toll-like receptor 4, a trigger for inflammation and innate immunity. *Biol. Reprod.* 78: 432–437.
25. Roberts, C. W., W. Walker, and J. Alexander. 2001. Sex-associated hormones and immunity to protozoan parasites. *Clin. Microbiol. Rev.* 14: 476–488.
26. García-Gómez, E., B. González-Pedrajo, and I. Camacho-Arroyo. 2013. Role of sex steroid hormones in bacterial-host interactions. *BioMed Res. Int.* 2013: 928290.
27. Bouman, A., M. J. Heineman, and M. M. Faas. 2005. Sex hormones and the immune response in humans. *Hum. Reprod. Update* 11: 411–423.
28. Hannah, M. F., V. B. Bajic, and S. L. Klein. 2008. Sex differences in the recognition of and innate antiviral responses to Seoul virus in Norway rats. *Brain Behav. Immun.* 22: 503–516.
29. Robinson, D. P., M. E. Lorenzo, W. Jian, and S. L. Klein. 2011. Elevated 17β-estradiol protects females from influenza A virus pathogenesis by suppressing inflammatory responses. *PLoS Pathog.* 7: e1002149.
30. Robinson, D. P., O. J. Hall, T. L. Nilles, J. H. Bream, and S. L. Klein. 2014. 17β-estradiol protects females against influenza by recruiting neutrophils and increasing virus-specific CD8 T cell responses in the lungs. *J. Virol.* 88: 4711–4720.
31. Karnam, G., T. P. Rygiel, M. Raaben, G. C. Grinwis, F. E. Coenjaerts, M. E. Ressing, P. J. Rottier, C. A. de Haan, and L. Meyaard. 2012. CD200 receptor controls sex-specific TLR7 responses to viral infection. *PLoS Pathog.* 8: e1002710.
32. Robinson, D. P., S. A. Huber, M. Moussawi, B. Roberts, C. Teuscher, R. Watkins, A. P. Arnold, and S. L. Klein. 2011. Sex chromosome complement contributes to sex differences in coxsackievirus B3 but not influenza A virus pathogenesis. *Biol. Sex Differ.* 2: 8.
33. Straub, R. H. 2007. The complex role of estrogens in inflammation. *Endocr. Rev.* 28: 521–574.
34. Malkin, C. J., P. J. Pugh, R. D. Jones, D. Kapoor, K. S. Channer, and T. H. Jones. 2004. The effect of testosterone replacement on endogenous inflammatory cytokines and lipid profiles in hypogonadal men. *J. Clin. Endocrinol. Metab.* 89: 3313–3318.
35. Peretz, J., A. Pekosz, A. P. Lane, and S. L. Klein. 2016. Estrogenic compounds reduce influenza A virus replication in primary human nasal epithelial cells derived from female, but not male, donors. *Am. J. Physiol. Lung Cell. Mol. Physiol.* 310: L415–L425.
36. Baccala, R., M. J. Welch, R. Gonzalez-Quintial, K. B. Walsh, J. R. Teijaro, A. Nguyen, C. T. Ng, B. M. Sullivan, A. Zarpellon, Z. M. Ruggeri, et al. 2014. Type I interferon is a therapeutic target for virus-induced lethal vascular damage. *Proc. Natl. Acad. Sci. USA* 111: 8925–8930.
37. Whitfield, J., T. Littlewood, and L. Soucek. 2015. Tamoxifen administration to mice. *Cold Spring Harb. Protoc.* 2015: 269–271.
38. Shaw, A. C., D. R. Goldstein, and R. R. Montgomery. 2013. Age-dependent dysregulation of innate immunity. *Nat. Rev. Immunol.* 13: 875–887.
39. Klein, S. L. 2011. Implications of X-linked gene regulation for sex differences in disease pathogenesis (comment on DOI 10.1002/bies.201100047). *BioEssays* 33: 789–790.
40. Klein, S. L. 2000. The effects of hormones on sex differences in infection: from genes to behavior. *Neurosci. Biobehav. Rev.* 24: 627–638.
41. Brownstein, D. G., and L. Gras. 1995. Chromosome mapping of Rmp-4, a gonad-dependent gene encoding host resistance to mousepox. *J. Virol.* 69: 6958–6964.
42. Meier, A., J. J. Chang, E. S. Chan, R. B. Pollard, H. K. Sidhu, S. Kulkarni, T. F. Wen, R. J. Lindsay, L. Orellana, D. Mildvan, et al. 2009. Sex differences in the Toll-like receptor-mediated response of plasmacytoid dendritic cells to HIV-1. *Nat. Med.* 15: 955–959.
43. Seillet, C., S. Laffont, F. Trémollières, N. Rouquié, C. Ribot, J. F. Arnal, V. Douin-Echinard, P. Gourdy, and J. C. Guéry. 2012. The TLR-mediated response of plasmacytoid dendritic cells is positively regulated by estradiol in vivo through cell-intrinsic estrogen receptor α signaling. *Blood* 119: 454–464.
44. Murphy, A. J., P. M. Guyre, and P. A. Pioli. 2010. Estradiol suppresses NF-kappa B activation through coordinated regulation of let-7a and miR-125b in primary human macrophages. *J. Immunol.* 184: 5029–5037.
45. Zhang, X., L. Wang, H. Zhang, D. Guo, Z. Qiao, and J. Qiao. 2001. Estrogen inhibits lipopolysaccharide-induced tumor necrosis factor-alpha release from murine macrophages. *Methods Find. Exp. Clin. Pharmacol.* 23: 169–173.
46. Roberts, A., D. Deming, C. D. Paddock, A. Cheng, B. Yount, L. Vogel, B. D. Herman, T. Sheahan, M. Heise, G. L. Genrich, et al. 2007. A mouse-adapted SARS-coronavirus causes disease and mortality in BALB/c mice. *PLoS Pathog.* 3: e5.
47. Cousins, S. W., M. E. Marin-Castaño, D. G. Espinosa-Heidmann, A. Alexandridou, L. Striker, and S. Elliot. 2003. Female gender, estrogen loss, and Sub-RPE deposit formation in aged mice. *Invest. Ophthalmol. Vis. Sci.* 44: 1221–1229.
48. Heil, F., H. Hemmi, H. Hochrein, F. Ampenberger, C. Kirschning, S. Akira, G. Lipford, H. Wagner, and S. Bauer. 2004. Species-specific recognition of single-stranded RNA via toll-like receptor 7 and 8. *Science* 303: 1526–1529.